Numerical simulation of twin-screw expander and its effect on the performance of ORC system

Lantian Ji1[0000-0001-9910-9150], Zhilong He1[0000-0002-2531-1310], Xiao Wang1, Ziwen Xing1[0000-0002-2750-5039]

1 Xi'an Jiaotong university. Xi'an, Shaanxi Province 710049, China
jlt364844834@stu.xjtu.edu.cn.

Abstract. For improving the expander modeling progress of the numerical simulation to get higher accuracy and obtaining its influence on the organic Rankine cycle system, this paper used a structured dynamic grid generation method based on expander rotor node mapping and a grid update technology of node migration with rotor profile to mesh by Twinmesh and Ansys and calculated the model by CFX. At the same time, the entire organic Rankine cycle system model was established. The results show that the simulation results are more suitable for the actual working process and has about 3% relative error, which is less than the reference literature results. The expander throttling loss and pre-expansion at the suction port reduce the overall performance of the expander, the leakage of tip clearance is the most serious, which should be controlled in the structure design of twin-screw expander. The indicated efficiency decreases with the increase of rotating speed and increases first and then decreases with the increase of suction pressure and discharge pressure due to over-expansion and under-expansion. The mass flow rate increases with the increase of suction pressure and rotating speed. The thermal efficiency and output power of the organic Rankine cycle system increase with increase of suction pressure and expander's rotating speed, and decrease with the increase of discharge pressure. This paper can provide a good reference for the theoretical simulation method exploration, optimal design of twin-screw expander and organic Rankine cycle system.

Keywords: Twin-screw expander, Organic Rankine Cycle(ORC), Numerical simulation, Dynamic mesh.

1 Introduction

The organic Rankine cycle (ORC) uses low-boiling organics as the working fluid, which makes it show great advantages of less heat required in the evaporation process and small circulation pressure ratio, etc. in below 300°C waste heat recovery. As the core component of the ORC system, the expander has a great impact on the power generation and system performance. Twin-screw expanders have significant advantages compared with the others, such as fewer wearing parts, high volume coefficient, low failure rate and so on. However, its actual working process is a complex, comprehensive, and transiently completed variable-mass thermodynamic process. To establish a fusion mathematical model of the thermal performance and dynamic characteristics calculation of the working process is the key and foundation of research on twin-screw expander.

In terms of working process simulation, Iva Papes[1] et al. used CFD to analyze the internal flow field of two twin-screw expanders under different pressure ratios and rotating speeds, and constructed a three-dimensional structured grid by solving the Laplace problem. The results show that the mass flow rate of working fluid increases with the increase of pressure or rotating speed, the leakage decreases with the increase of rotating speed, and the throttling loss at the inlet of the expander cause a large pressure drop.Yuanqu Qi[2,3] et al. established a three-dimensional geometric model and thermodynamic model of the twin-screw expander. The results indicated that throttling, pressure drop and leakage loss are the main factors affecting the efficiency of the twin-screw expander. The large suction pressure loss and the long sealing line makes the leakage serious in the initial stage of expansion. The leakage, throttling and pressure drop loss increase with the increase of suction pressure and the decrease of rotating speed. Professor Stosic, Smith and Kovacevic of City University, UK[4-6] also have rich experience in the theoretical and experimental research of twin-screw compressors and expanders for power generation. They constructed and compared the one-dimensional and three-dimensional performance calculation models, introduced the geometric characteristics, design concepts and some design cases of the twin-screw expander. Wu Gaojie[7] used CFD to numerically simulate the internal flow field of the designed twin-screw expander and Ansys Workbench to simulate the dynamic characteristics of the rotors. The simulation results show that the temperature change of the medium and low temperature heat source has little effect on the operation of the expander. The large pressure difference at the suction port and the too fast gas flow when passing through the meshing gap result in a negative pressure phenomenon. Hao Tang[8]used Matlab to establish the working process and ORC system model of the twin-screw expander, optimized the leakage model of the expander, and analyzed the variation law of the twin-screw expander core parameters under variable working conditions.

From the above research content, the simulation of the working process of the twin-screw expander needs to consider the effects of the axial clearance and the radial clearance on the performance of the expander at the same time. However, there are still three major problems that need to be optimized and improved: 1) The size of the tip clearance and inter-tooth clearance is three orders of magnitude different from the size of the working chamber. The entire computational domain has a large scale span. Meshing is difficult but very critical to the accuracy of results; 2) The working chamber is a dynamic flow domain. Meshing requires moving boundaries; 3) The constant exhaust pressure at the gas pipe port is usually given as the boundary condition in numerical simulation of the twin-screw expander, and the influence of the pipeline is not considered, which does not match the actual situation. In addition, the exhaust process of the twin-screw expander is discontinuous and has obvious periodicity, which makes the pressure in the exhaust pipe fluctuate. In order to solve the above problems, this paper optimized and improved the modeling process of the twin-screw expander by using a structured dynamic grid generation method based on expander rotor node mapping and a grid update technology of node migration with rotor profile. The simulation results are closer to the actual operating state. At the same time, the entire ORC system model was established, and the influence of the working law of the twin-screw expander on the performance of the ORC system under variable working conditions was analyzed. The research results can provide a good reference for the theoretical simulation method exploration, optimal design of twin-screw expander and its adaptation to the ORC system.

2 Methodology

2.1 Numerical Simulation of the Twin-screw Expander Working Process

The structural parameters of the twin-screw expander are shown in Table 1. The twin-screw expander female and male rotor models and the twin-screw expander domain modelare shown in Fig.1.

Table 1. The structural parameters of the twin-screw expander.

Parameter name	Value
Rotor length/mm	140
Male rotor helical pitch/mm	210
Female rotor helical pitch/mm	294
Inner volume ratio	2.3
Center distance of the male and female rotor/mm	108.2
External diameter of the male rotor/mm	143
External diameter of the female rotor/mm	123
Number of the male rotor teeth	5
Number of the female rotor teeth	7

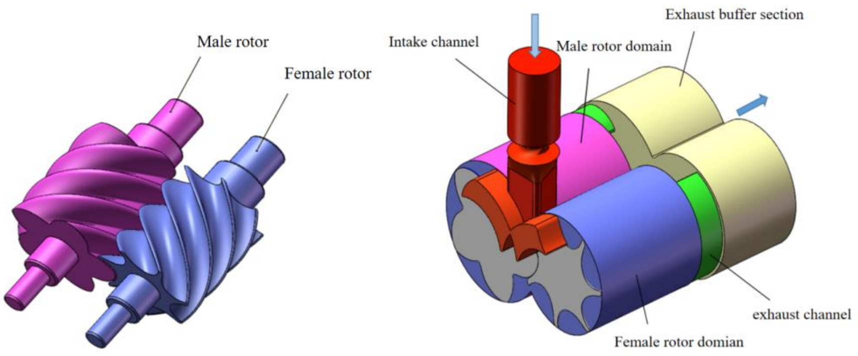

Fig.1. The twin-screw expander female and male rotor models and the twin-screw expander domain model.

Grid Generation. The calculation area was divided into static domain and dynamic domain for meshing respectively. The static domain includes three parts: the inlet pipeline domain, the exhaust pipeline domain and the exhaust buffer domain. The generated mesh is shown in Fig.2. Unstructured tetrahedral meshes was used for both the inlet and the exhaust pipeline domain, and some meshes connected to the rotor dynamic domain were refined to 0.3mm. The exhaust buffer domain adopted structured hexahedral meshes. The mesh element nodes can be connected in any form.

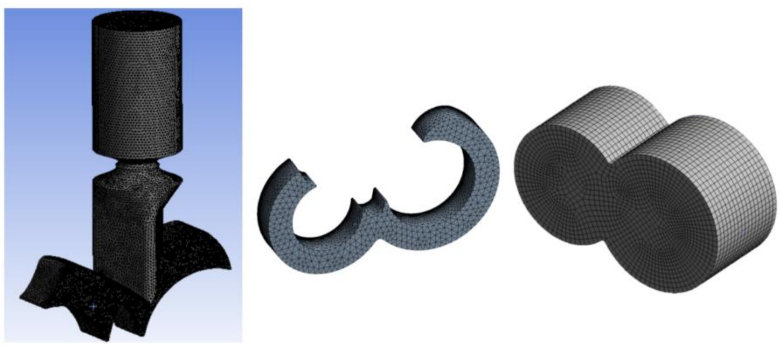

Fig.2. The generated static domain mesh.

The expansion working chamber domain is the dynamic domain, whose 2D structured quadrilateral grid was generated by TwinMesh. The 3D structured mesh of the working chamber is shown in Fig.3. A 5-layer mesh was uniformly generated at the axial clearance. The mesh density near the wall is higher, and gradually becomes sparser towards the middle of the working chamber in a certain proportion to control the overall mesh number. The minimum angle of the partial mesh is 48.74°, which is much larger than the lower limit 10°of the minimum angle set by the mesh quality detection. Therefore, the quality of the generated grid meets the simulation requirement, and the structured grid can transition smoothly. The mesh quality is good.

Fig.3. The 3D structured mesh of the working chamber.

In ANSYS-FLUENT, the grid is automatically updated according to the change of the boundary in each iteration. The quality of the generated mesh is difficult to guarantee, and the simulation speed is seriously affected. The dynamic grid node update method used in this paper is based on the structured grid point-to-point key frame dynamic grid update technology. From the previous moment to the next moment, the grid is updated according to the positions of the male and female rotors. This method overcomes the shortcomings of the above-mentioned traditional grid update method, which can generate high-quality and reasonable structured grids in cross-scale domain and avoid repeated grid updates to improve simulation solution efficiency.

Numerical Solution. In order to simplify the calculation, the working process was assumed: 1) The circulating working fluid is R245fa, and the dynamic viscosity coefficient is constant; 2) The twin-screw expander only exchanges mass with the external environment through the intake and exhaust ports, without considering the influence of the external leakage; 3) The influence of temperature change on the deformation of the expander is ignored. Both the rotor and the casing are rigid bodies during the working process. Ansys-CFX was used to solve the calculation and the shear stress transfer k-ω model in the Reynolds time-averaged method as the turbulent flow calculation model.

In this paper, the inlet pressure is 6.58bar, the exhaust pressure is 2.9bar, and the rotating speed is 1100 r·min^{-1} as an example. The inlet temperature is 74℃. The export pressure boundary condition is determined by the inlet pressure and expansion ratio, and the boundary is set to opening, that is, the fluid is allowed to enter and exit. The mesh independence verification is carried out to avoid the influence of the number of meshes, mesh quality and mesh structure on the simulation results. The results are shown in Fig.4.

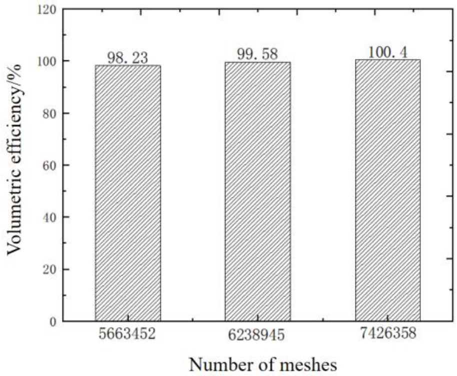

Fig.4. Mesh independence verification results.

2.2 Numerical Simulation of ORC System

The ORC system used R245fa as the working fluid. The Temperature-Entropy diagram of the ORC system is shown in Fig.5.

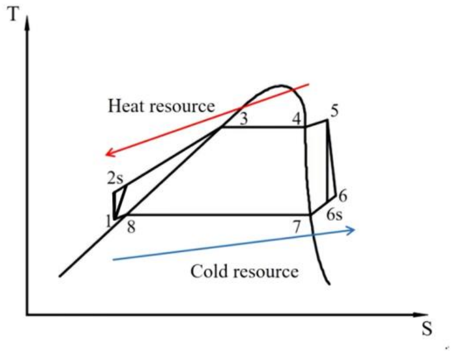

Fig.5. The Temperature-Entropy diagram of the ORC system.

The condenser and the evaporator are both corrugated plate type counter-flow heat exchangers. The basic assumptions are as follows: 1) The flow of the working fluid is one-dimensional homogeneous. The pressure keeps constant, and the mass flow remains unchanged. The pressure and temperature drop formed by the flow are not considered, that is, the momentum conservation equation is not considered. The stable flow satisfies the continuity equation, and only the energy conservation equation is considered; 2) The flow of heat source water and cooling water is one-dimensional. 3) Ignore the contact thermal resistance and heat conduction thermal resistance caused by the plates, but only consider the convection thermal resistance; 4) The heat exchanger is divided into subcooling, superheating, and two-phase calculation areas. The heat leakage is not zero. The ratio of the heat exchange between working fluid and water in each calculation area is the same but not 1.

$$Q = m\alpha(T_{in} - T_{\text{out}}) = m(h_{in} - h_{out}) \tag{1}$$

$$\frac{T_{wc\_out} - T_{w3}}{h_6 - h_7} = \frac{T_{w3} - T_{w2}}{h_7 - h_8} = \frac{T_{w2} - T_{wc\_in}}{h_8 - h_1} = c_Q \tag{2}$$

$$c_{(sh,sc,tp)} = \frac{\dfrac{\Delta h_{(sh,sc,tp)}}{\Delta T_{(sh,sc,tp)}}}{\Sigma \dfrac{\Delta h}{\Delta T}} \tag{3}$$

$$Nu_{sp} = 0.023 \cdot \mathrm{Re}_{sp}^{0.8} \cdot \mathrm{Pr}_{sp}^{n} \tag{4}$$ [9]

Among them, n is taken as 0.3 when the working fluid is cooled and 0.4 when heated.

$$\mathrm{Re}_{sp} = \frac{u_r \cdot d}{\nu} \tag{5}$$

$$Nu_{eq} = C \cdot \mathrm{Re}_{eq}^{m} \cdot \mathrm{Pr}_{l}^{n} \tag{6}$$

$$\mathrm{Re}_{eq} = m_r[(1-x) + x(\frac{\rho_l}{\rho_g})^{0.5}]\frac{d}{\nu_l} \tag{7}$$ [10]

$$\alpha = \frac{Nu \cdot k}{d} \tag{8}$$

$$W_p = m_r(h_2 - h_1) \tag{9}$$

The inlet superheat degree of the expander is a assumed value (iterative calculation) at 0~10℃. The temperature, pressure and mass flow rate of the expander at the expander outlet were all provided by the thermodynamic simulation results of the expander. The fitting formulas of the above thermodynamic parameters for the evaporation and condensation temperature are given. In this way, the TwinMesh simulation results of the expander are brought into the system for simulation.

$$W_{\exp} = m_r(h_5 - h_6) \tag{10}$$

$$\eta_{sys} = \frac{W_{\exp} - W_p}{Q_{evap}} \tag{11}$$

The ORC system and heat exchanger block diagram are shown in Fig.6. Programming and calculations were implemented in Matlab.

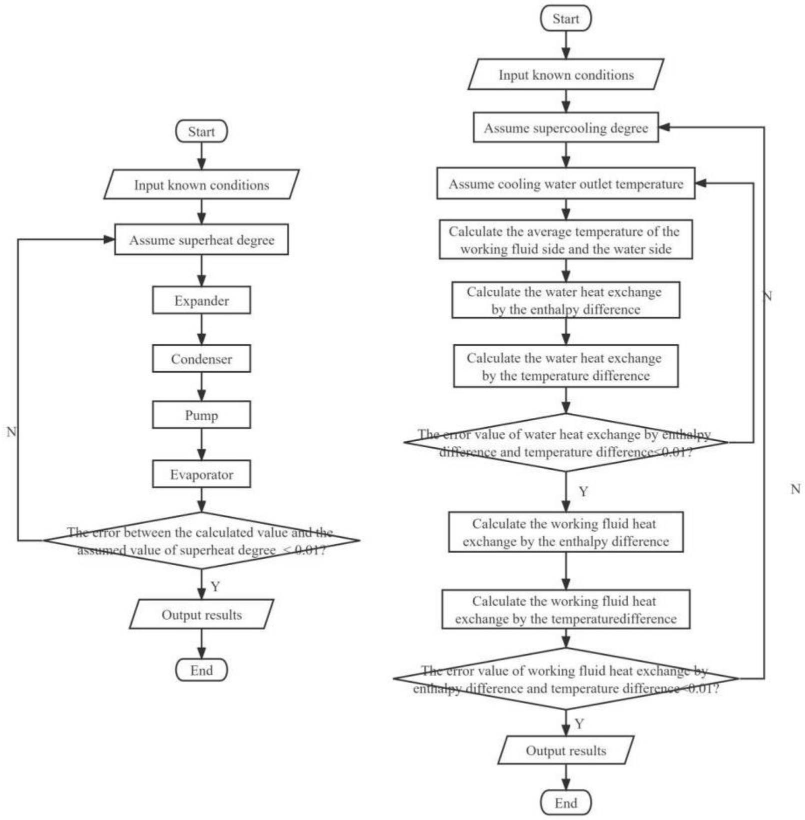

Fig.6. The ORC system and heat exchanger block diagram.

3 Results and Discussion

In this paper, three sets of experimental data from the literature[8] were selected to verify the models of the ORC system and the twin-screw expander. The operating point parameters are shown in Table 2 and Table 3. The model error results are shown in Fig.7. The left side of the figure is the output power error value of the twin-screw expander, and the right side is the ORC system error value. It can be seen that the average error is about 3%, which is less than the results in the reference literature.

Table 2. Expander model verification condition parameters.

Serial number	n_{exp}	P_{in_exp}	P_{out_exp}	T_{in_exp}
1	1100	658	290	72.9
2	1300	658	290	72.9
3	1500	658	290	72.9

Table 3. ORC system model verification condition parameters.

Serial number	n_{exp}	P_{in_exp}	T_e	P_{out_exp}	T_{sh}	T_c
1	1100	658	72.9	290	0	44
2	1500	658	72.9	290	1.5	44
3	1100	590	68.8	290	0	44

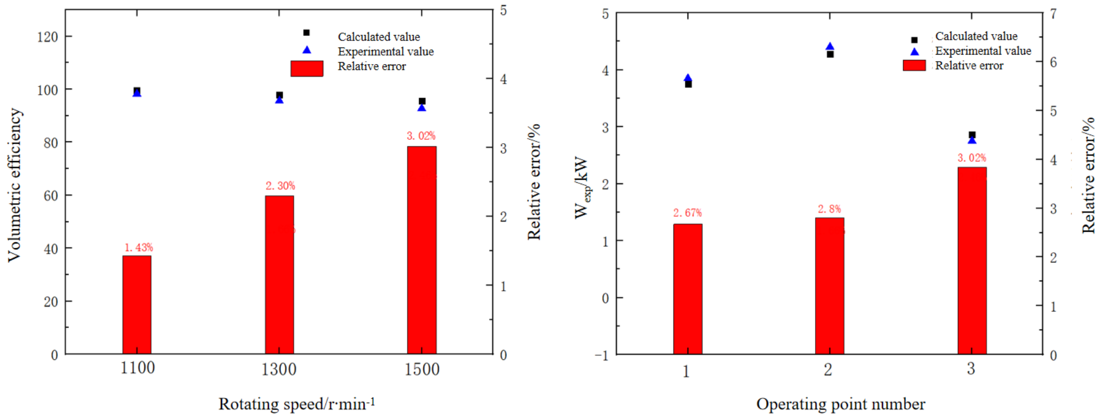

Fig.7. The model error results.

This section selected the number 1 working condition in Table 2 to analyze the twin-screw expander. The geometric parameters of the model are shown in Table 4. The variation of pressure in a working chamber with the rotating angle of the male rotor is shown in Fig.8.

Table 4. Twin-screw expander model geometric parameters.

Parts	Number of teeth	θ	l_{ra}	δ_{tc}	δ_{cbt}	δ_{ec}
Male rotor	5	240	140	0.1	0.15	0.1
Female rotor	7	171.43				

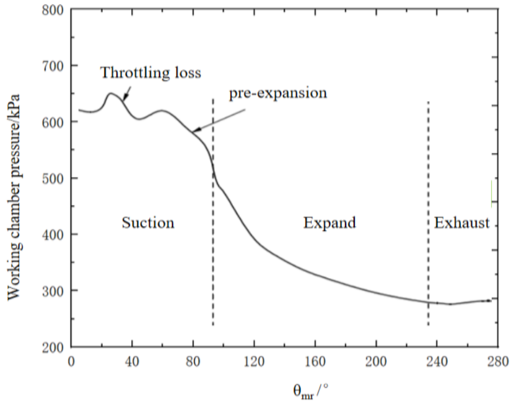

Fig.8. The variation of pressure in a working chamber with the rotating angle of the male rotor.

As shown in Fig.8, since the pre-expansion occurs at the moment when the working chamber is connected to the suction pipeline, the output work of the pre-expansion is not effectively recovered, which reduces the working efficiency of the twin-screw expander. Both throttling loss and pre-expansion are closely related to the shape of the suction port, so optimizing the shape of the suction port can greatly improve the performance of the twin-screw expander. The surface pressure distribution of the male and female rotors is shown in Fig.9. Along the axial direction of the rotors, the pressure on the surfaces decreases first and then increases slightly from the suction end face to the discharge end face, mainly because the given pressure boundary condition of the exhaust port is greater than the theoretical value. Therefore, after the gas in the expansion chamber reaches the exhaust end face, the pressure value is less than it given by the exhaust port, and the gas outside the exhaust end face flow back into the expansion chamber.

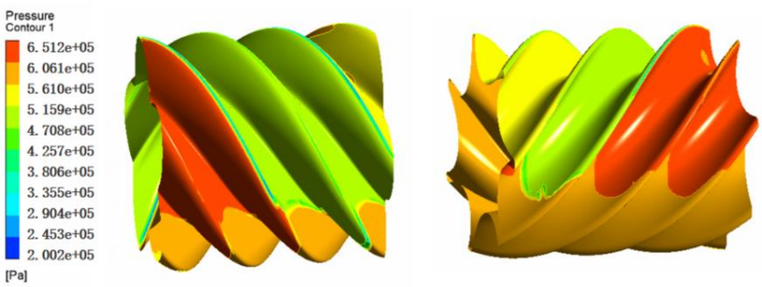

Fig.9. The surface pressure distribution of the male and female rotors.

The rotor axial direction section Z=5mm, Z=70mm and Z=135mm were choose to draw cross-sectional pressure cloud diagram. The pressure cloud diagrams at the three sections is shown in Fig.10. It can be seen that the pressure distribution in each expansion chamber is relatively uniform, the pressure at the suction end face is the highest, and gradually decreases along the axial direction of the rotor. A minimum value of 200kPa is reached. However, in the simulated working condition, the pressure boundary condition at the exhaust port is 290kPa, so there is a large degree of turbulence in this area, which outputs the exhaust noise.

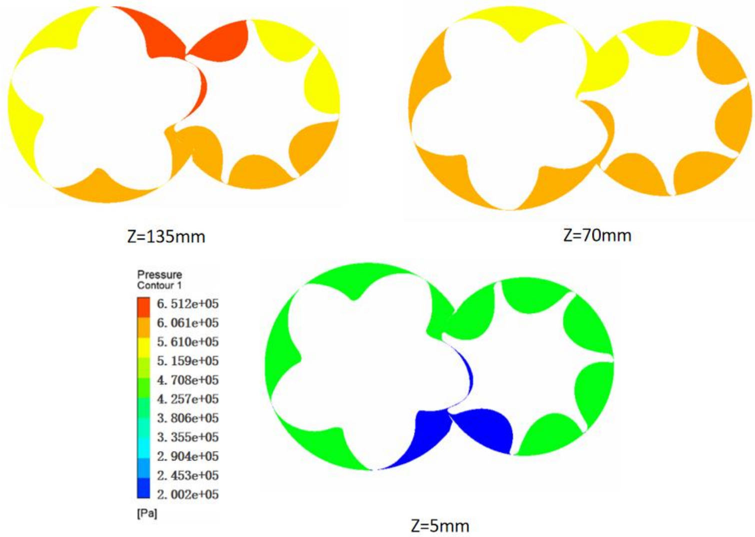

Fig.10. The pressure cloud diagrams at the three sections.

The velocity vector diagram of the rotors domain and the velocity vector diagram of the rotor section (Z=135mm) are shown in Fig.11. The fluid velocity distribution in each chamber is relatively stable, and there is no region that produces drastic changes. However, the velocity of the leaking gas at the tip clearance and the inter-tooth clearance is an order of magnitude larger than that in the expansion chamber. The pressure difference between chamber 1 and chamber 2 near the suction end face is the largest, reaching 650kPa. Therefore, the maximum flow velocity is at the tip clearance and the inter-tooth clearance. The leakage of gas at the gap will greatly affect the efficiency of the expander, so it is necessary to reduce the tip and inter-tooth clearances as much as possible under the condition of ensuring the normal operation of the expander. The value and direction of the fluid velocity on each section are basically the same, and there are only slight differences in some areas, which means that the flow of the working fluid in the expansion chamber is relatively stable. The speed of the rotor meshing area increases, which is due to the turbulent flow here. The leakage at the tip clearance is the most serious. The fluid velocity between the tip circle part of the rotors and the twin-screw body is faster, because the pressure difference between the two ends of the axial direction is large. Reasonable setting of the meshing clearance and the clearance between the tip circle and the casing directly affects the volumetric efficiency of the expander. Therefore, when designing and improving the expander, they should be designde properly to avoid unnecessary leakage.

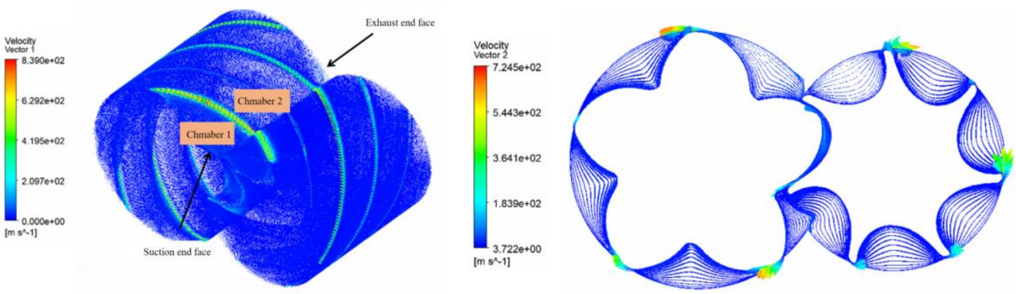

Fig.11. The velocity vector diagram of the rotors domain and the velocity vector diagram of the rotor section (Z=135mm).

The variation of the expander performance parameters with the speed is shown in Fig.12. When the rotating speed increases, the suction pressure loss increases gradually. When the rotating speed is greater than 1300 r·min^{-1}, the pressure loss has a significant increase. This is because the losses increase caused by wall friction and throttling with the flow velocity increase.When the speed reaches 1900 r·min^{-1}, the pressure in the working chamber cannot even reach the given suction pressure. The volumetric efficiency gradually decreases, which is mainly due to the influence of suction pressure loss and clearance leakage. When the rotating speed is less than 1500 r·min^{-1}, the clearance leakage has a greater influence on the flow rate of the expander. But when the rotating speed is greater than 1500 r·min^{-1}, the suction pressure loss has a greater influence on the flow rate of the expander, and the volumetric efficiency decreases rapidly. The indicated efficiency decreases with increasing rotating speed, mainly due to suction pressure loss and leakage both reducing the actual output power of the expander. The mass flow rate of the working fluid increases with the increase of the rotating speed. With the increase of the rotating speed, the output power of the expander increases gradually, but when the speed is greater than 1500 r·min^{-1}, the increase of the output power decreases obviously. When the rotating speed reaches 1900 r·min^{-1}, the output power drops significantly, mainly because the increase of the rotating speed makes the suction pressure loss increase. The actual pressure difference between the suction and exhaust of the expander decreases, and the ability to output work also decreases.

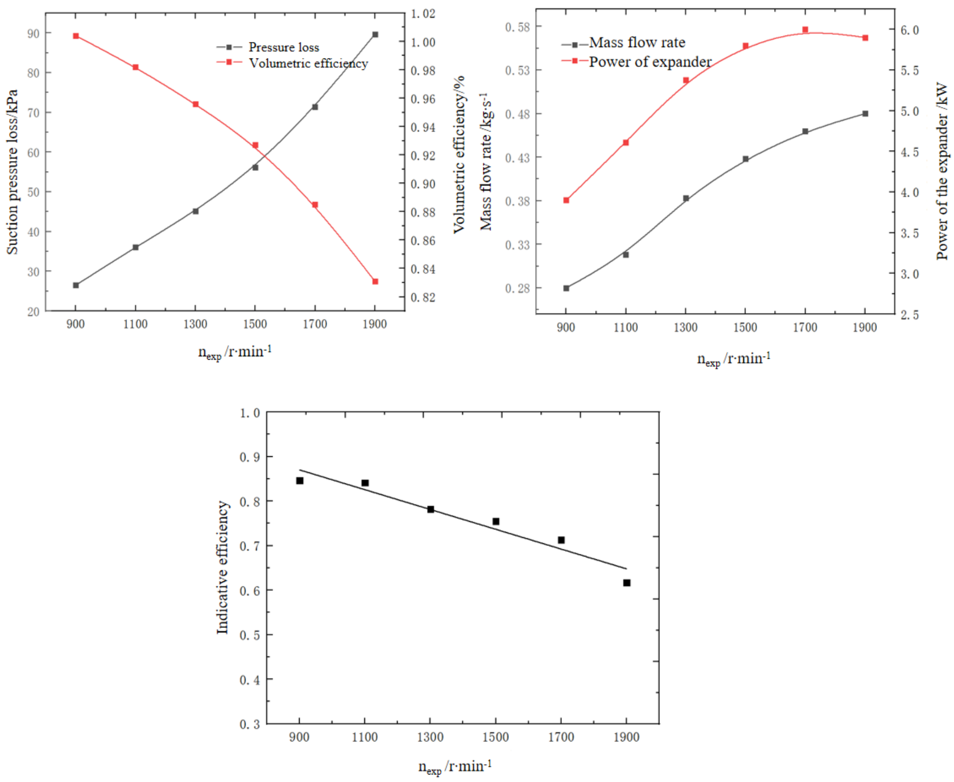

Fig.12. The variation of the expander performance parameters with the rotating speed(The exhaust pressure: 290kPa; The inlet pressure: 658kPa; The condensation temperature: 44℃; The evaporation temperature: 72.9℃).

The variation of the expander performance parameters with the suction pressure is shown in Fig.13. As the suction pressure rises, the suction pressure loss also increases linearly. This is because when the suction pressure increases, the velocity of the working fluid at the suction port increases, the friction with the wall becomes more intense, and the energy loss is more. Overall, the increase in suction pressure loss is not large. Due to the over-expansion and under-expansion of the expander, the indicated efficiency is reduced, and the actual output power of the expander is affected. The working fluid flow rate basically increases linearly, because when the suction pressure increases, the suction pressure loss also increases, but at the same time, the working fluid density is higher, resulting in a larger mass flow rate. Although the indicated efficiency of the expander will be negatively affected by over-expansion or under-expansion, due to the steady increase in the working fluid flow rate and suction temperature, the working fluid entering the expander with a lot of energy, which promotes the stable increase of the output power of the expander.

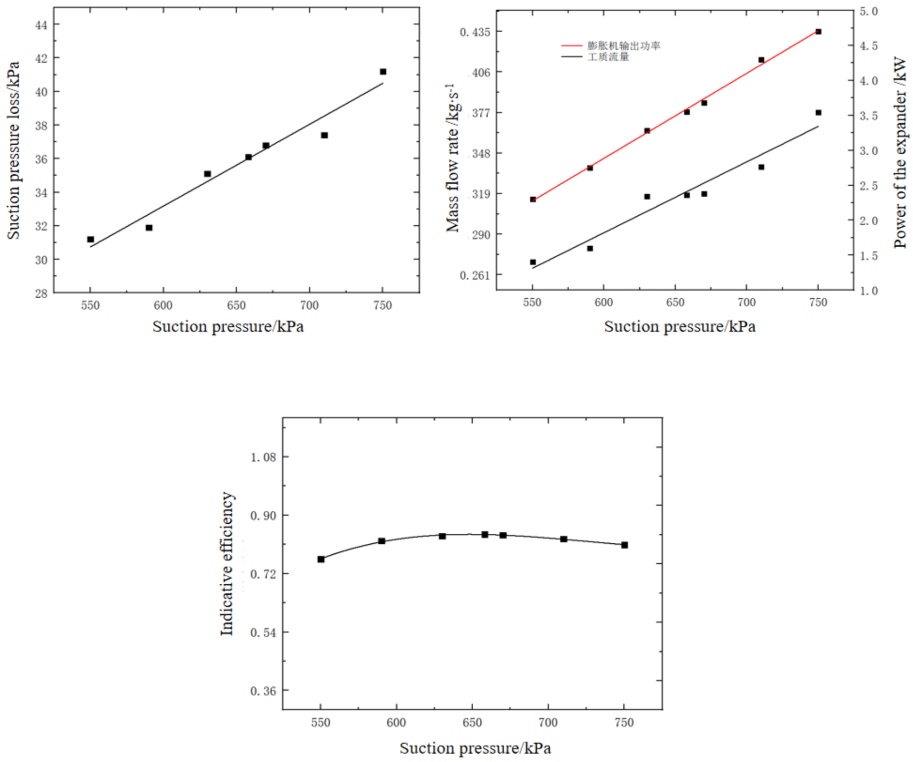

Fig.13. The variation of the expander performance parameters with the suction pressure(The exhaust pressure: 290kPa; The condensation temperature: 44℃; The rotating speed: 1100 r·min^{-1}).

The variation of the expander performance parameters with the exhaust pressure is shown in Fig.14. When the exhaust pressure increases, the suction pressure loss remains basically the same, then when the inlet working fluid parameters are the same, the pressure at the rotor inlet is basically unchanged. The change of the exhaust pressure will not affect the suction state of the expander. The working fluid flow state in the working chamber will not change greatly. A drop in indicated efficiency meas that either under-expansion or over-expansion of the expander will reduce the performance of the expander. The change of exhaust pressure has no great influence on the working fluid flow rate, and the output power will decrease linearly with the increase of exhaust pressure. This is because the increase in exhaust pressure means that the condensation temperature increases, and the enthalpy difference between the inlet and exhaust ports of the expander decreases.

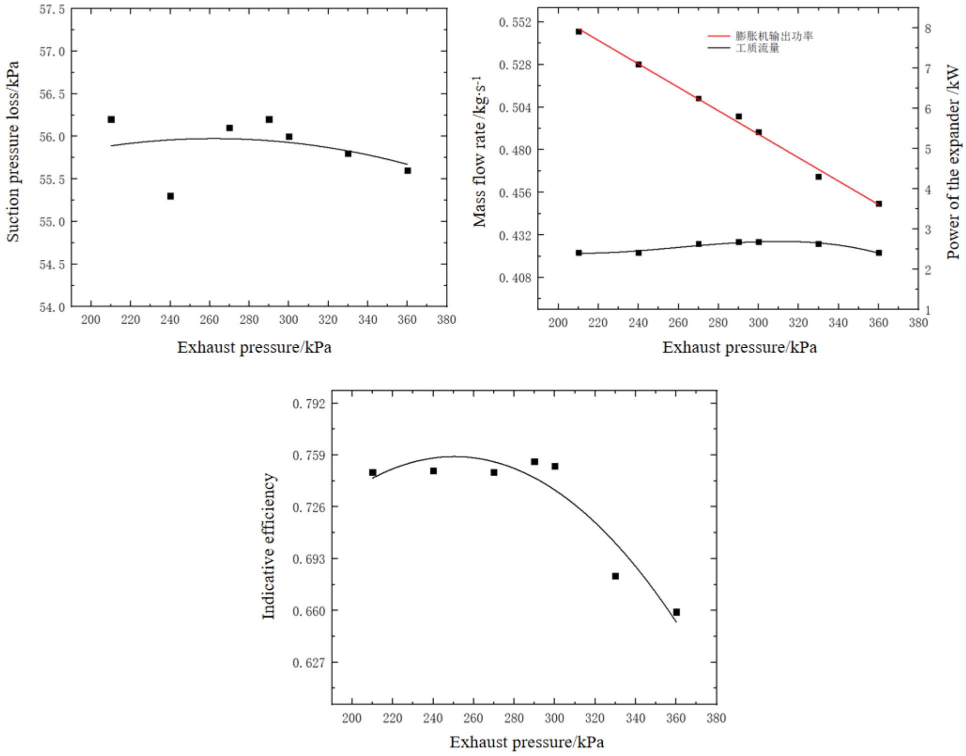

Fig.14. The variation of the expander performance parameters with the exhaust pressure(The suction pressure: 658kPa; The suction temperature: 73℃; The rotating speed: 1500 r·min^{-1}).

The variation of system parameters with expander rotating speed, suction temperature and discharge pressure is shown in Fig.15. When the rotating speed of the expander increases, the output power of the system gradually increases when the speed is less than 1700 r·min^{-1}, but the growth is slow. That is because the increase of the rotating speed leads to an increase in the mass flow rate of the expander. The pump efficiency does not change much, and the indicated efficiency of the expander gradually decreases with the increase of the rotating speed. The evaporation temperature, condensation temperature, and superheat degree remain unchanged, the theoretical output power of the expander increases. The actual output power of the expander is the product of the theoretical output power and the indicated efficiency, but the increase of mass flow rate is greater than the decrease of indicated efficiency, so the actual output power of the expander will increase with the rotating speed. In addition, the change of pump power consumption is small, so the thermal efficiency of the system will decrease as the speed increases. When the rotating speed is greater than 1700 r·min^{-1}, the increase of pump power consumption is greater than the increase of output power of the expander, so the output power of the system will show a downward trend.

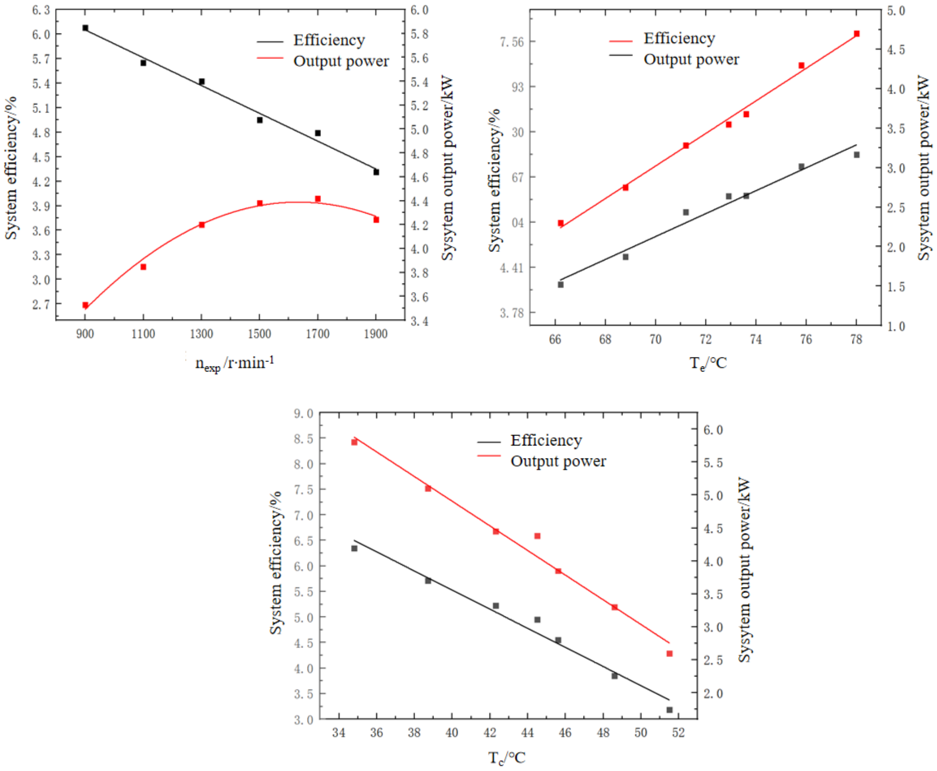

Fig.15. The variation of system parameters with expander performance parameters.

When the evaporation temperature increases, the suction temperature of the expander increases, and the output power of the system gradually increases. This is because the working fluid remains in a saturated gas state, and the suction pressure of the expander also increases correspondingly with the increase of the evaporation temperature. The indicated efficiency of the expander increases slightly with increasing evaporation temperature. The increase in mass flow makes the output power of the expander gradually increase, and the pump power does not change much, so the output power of the system also gradually increases. The thermal efficiency of the system gradually increases because the two-phase area in the evaporator accounts for a large proportion. The increase of the evaporation temperature will reduce the heat exchange temperature difference of the evaporator. Although the mass flow rate increases, the increase of the heat exchange amount of the evaporator is still small, so the thermal efficiency of the system will increase with the increase of the suction temperature of the expander. When the exhaust pressure of the expander increases, the thermal efficiency and output power of the system gradually decrease. This is because the indicated efficiency, mass flow rate and output power decrease with the increase of the exhaust pressure. So the output power of the system also decreases. The decrease of the temperature difference in the evaporator reduces the heat exchange amount, but which is smaller than that of the output power, so that the thermal efficiency of the system decreases with the increase of the exhaust pressure of the expander.

4 Conclusions

In this paper, the working process of the twin-screw expander was simulated by CFD. A complete three-dimensional numerical model was established, and the radial and axial leakage were considered. A structured dynamic mesh generation method based on the expander rotor node mapping and a mesh update technology in which the nodes migrated with the rotor profile were uesd. It is helpful to decrease the relative error and be closer to the actual working state. The problem of cross-scale dynamic grid generation of the non-contact twin-screw expander can be solved. In addition, the ORC system mathematical model was constructed and solved by using R245fa as the working fluid. The main results are as follows, which support great reference for design, troubleshooting, experimental study and product development of the twin-expander and ORC system:

1) The simulation results were compared with the experimental results of the literature. The relative error is about 3%, indicating that the mathematical model established in this paper can accurately simulate the ORC system and calculate the working characteristics of the expander. Through the analysis of the internal flow field of the expander, the variation law of the pressure in the working chamber with the angle of the male rotor was obtained. It was found that the shape of the suction orifice can cause throttling losses and pre-expansion during the suction process of the expander, thereby reducing the performance of the expander. Therefore, the design of the suction port should be optimized in the forward design of the twin-screw expander.

2) The analysis of the pressure nephogram and velocity vector diagram of the expander rotor domain shows that the pressure gradient changes the largest at the tip clearance near the suction end face and so as to the flow velocity. That indicates that the leakage is the most serious at the tip clearance. Therefore, in the structural design of the twin-screw expander, the size of the tip clearance should be controlled.

3) When the speed of the expander is low, the leakage has a greater impact on the performance of the expander. When the speed is higher than a certain value, the suction throttling loss caused by the increase of the speed has a greater impact on the performance of the expander. When the internal volume ratio is constant, if the suction air pressure or exhaust pressure deviates from the design value, the expander is in a state of over-expansion or under-expansion, reducing the overall performance of the expander. The indicated efficiency increases first and then decreases with the increase of suction pressure and exhaust pressure. Therefore, in the actual operation of the expander, the appropriate rotating speed, suction pressure and exhaust pressure should be matched to avoid over-expansion or under-expansion.

4) The thermal efficiency and output power of the system increase by about 0.3% and 0.43kW respectively for every 40kPa increase in suction pressure. The thermal efficiency and output power increase with the increase of rotating speed. At this time, the system efficiency is 4.79%, and the output power is 4.42kW. The thermal efficiency and output power decreases with the increase of the exhaust pressure. When the exhaust pressure is 360kPa, the efficiency and output power values are 3.19% and 2.6kW respectively. Therefore, it is necessary to select the appropriate expander speed, suction temperature and discharge pressure to adapt the ORC system to optimize the system performance.

References

1. Papes I, Degroote J, Vierendeels J. New insights in twin-screw expander performance for small scale ORC systems from 3D CFD analysis[J]. Applied Thermal Energy. 2015,91: 535-546.
2. Yuanqu Qi, Yuefeng Yu. Thermodynamic Simulation on the Performance of Twin-screw Expander Applied in Geothermal Power Generation[J]. Energies. 2016, 9: 694-703.
3. Yuanqu Qi, Yuefeng Yu. Numerical Simulation and Analysis of Leakage Process of Twin-screw Expander[J]. Journal of Shanghai Jiaotong University. 2016, 4(50): 496-501.

4. Kovacevic A, Stosic N, Smith I. Screw Compressors: Three Dimensional Computational Fluid Dynamics and Solid Fluid Interaction[J]. Springer Science & Business Media. 2007.
5. Smith I, Stosic N, Kovacevic A. Power Recovery From Low Grade Heat by Means of Screw Expanders[J]. Elsevier. 2014: 13-58.
6. Stosic N, Smith I, Kovacevic A. Screw Compressors: Mathematical Modelling and Performance Calculation[J]. Springer Science & Business Media. 2005: 49-75.
7. Gaojie Wu. Structural Design and Dynamic Performance Research of Medium and Low Temperature Twin-screw expander[D]. Yangzhou: Yangzhou University. 2017.
8. Hao Tang. Research on characteristics of twin-screw expander and performance of organic Rankine cycle system[D]. Xi'an: Xi'an Jiaotong university. 2016.
9. Shiming Yang, Wenquan Tao. Heat transfer[M]. Beijing:Higher Education Press. 2006.
10. Carlos A. Dorao, Maria Fernandino. Simple and general correlation for heat transfer during flow condensation inside plain pipes[J]. International Journal of Heat and Mass Transfer. 2018(122): 290-305.